Novel and Robust Transplantation Reveals the Acquisition of Polarized Processes by Cortical Cells Derived from Mouse and Human Pluripotent Stem Cells

Fumiaki Nagashima,[1] Ikuo K. Suzuki,[2] Atsunori Shitamukai,[3] Haruko Sakaguchi,[4] Misato Iwashita,[1] Taeko Kobayashi,[5] Shigenobu Tone,[6] Kazunori Toida,[1] Pierre Vanderhaeghen,[2,7] and Yoichi Kosodo[1]

Current stem cell technologies have enabled the induction of cortical progenitors and neurons from embryonic stem cells (ESCs) and induced pluripotent stem cells in vitro. To understand the mechanisms underlying the acquisition of apico-basal polarity and the formation of processes associated with the stemness of cortical cells generated in monolayer culture, here, we developed a novel in utero transplantation system based on the moderate dissociation of adherens junctions in neuroepithelial tissue. This method enables (1) the incorporation of remarkably higher numbers of grafted cells and (2) quantitative morphological analyses at single-cell resolution, including time-lapse recording analyses. We then grafted cortical progenitors induced from mouse ESCs into the developing brain. Importantly, we revealed that the mode of process extension depends on the extrinsic apico-basal polarity of the host epithelial tissue, as well as on the intrinsic differentiation state of the grafted cells. Further, we successfully transplanted cortical progenitors induced from human ESCs, showing that our strategy enables investigation of the neurogenesis of human neural progenitors within the developing mouse cortex. Specifically, human cortical cells exhibit multiple features of radial migration. The robust transplantation method established here could be utilized both to uncover the missing gap between neurogenesis from ESCs and the tissue environment and as an in vivo model of normal and pathological human corticogenesis.

Introduction

REMARKABLE ADVANCES in stem cell technologies now provide a methodology for inducing cortical neurons from pluripotent stem cells. Indeed, the generation of the different neuronal subtypes found within the six distinct layers of the mammalian cortex from embryonic stem cells (ESCs) and induced pluripotent stem cells (iPSCs) has been established in adherent monolayer culture systems [1–3] and self-organized cultures with polarized cytoarchitecture [4]. With these types of approaches, the entire neurogenic process, from undifferentiated stem cells to terminally differentiated neurons, can be tracked in the defined conditions of a culture dish. These culture systems are expected not only to offer an unlimited source of cortical neurons for clinical research into regenerative therapies and pharmacological screening for neurodegenerative diseases but also to provide novel strategies to answer fundamental questions of the brain's development and its disorders [5]. It has been demonstrated that terminally differentiated cortical neurons derived from mouse [6] and human [3] ESCs can integrate into mouse brain circuits. However, it is still largely unknown whether and to what extent undifferentiated neural progenitors or immature neurons generated in vitro integrate into germinal tissue and recapitulate the processes of physiological neurogenesis in vivo.

At least three subtypes of neural progenitors exist during corticogenesis in mammals: neuroepithelial/radial glial cells (also known as "apical progenitors"), intermediate (basal) progenitors, and outer subventricular zone (OSVZ) progenitors [7,8]. These neural progenitors exhibit differences with regard to both stemness, including self-renewal and multipotency, and cell biology, including their symmetric versus asymmetric mode of cell division and polarity.

[1]Department of Anatomy, Kawasaki Medical School, Kurashiki, Japan.
[2]ULB Neuroscience Institute (UNI), Institut de Recherches en Biologie Humaine et Moléculaire (IRIBHM), Université Libre de Bruxelles (ULB), Brussels, Belgium.
[3]Laboratory for Cell Asymmetry, RIKEN Center for Developmental Biology, Kobe, Japan.
[4]Department of Plastic and Reconstructive Surgery, Kawasaki Medical School, Kurashiki, Japan.
[5]Institute for Virus Research, Kyoto University, Kyoto, Japan.
[6]Department of Biochemistry, Kawasaki Medical School, Kurashiki, Japan.
[7]WELBIO, Université Libre de Bruxelles (ULB), Brussels, Belgium.

Notably, it has been proposed that the mode of cellular process extension is one of the key cytoarchitectural factors that characterizes these subtypes [7,8]. Apical progenitors, which are at the base of the neural progenitor lineage because they can generate all of the known subtypes of neural progenitors, as well as post-mitotic neurons [7,8], have two processes that extend in the apical and basal directions (the apical and basal processes, respectively) along the epithelial polarity of the brain tissue [9–12]. Intermediate progenitors, which lack self-renewing activity and generate two neurons through symmetric division, have no major processes [13–15]. OSVZ progenitors, which have self-renewing activity and generate neurons through asymmetric division, retain the basal process but lack the apical process [12,16–19]. Thus, the types of processes reflect the intrinsic differentiation status of each cortical progenitor subtype.

Because the presence of cellular processes correlates with the stemness of endogenous cortical progenitors, we asked whether ESC-derived cortical cells in the culture dish have the ability to extend their processes in a way that reflects their intrinsic differentiation status and the extrinsic environment of the tissue. To examine this question, one feasible approach is to analyze the morphology of ESC-derived cortical cells transplanted into a developing brain. To achieve this aim, we established a novel method of transplantation based on the dissociation of apical cellular junctions in the host tissue. With this method, we found not only that the efficiency of transplantation dramatically increased but also that the grafted cells exhibited a dispersed distribution in the host tissue, allowing us to assess their morphology quantitatively with single-cell resolution. We further addressed the significant question of whether cortical cells induced from ESCs in adherent monolayer culture have an ability to acquire polarized processes in response to the tissue environment by investigating their cytoarchitectures in the developing brain. Moreover, we documented that human-ESC-derived cortical cells are also incorporated into the developing mouse brain robustly, indicating that this experimental system could become a basis for future studies of human corticogenesis.

Materials and Methods

Animals

Transgenic mice expressing the *Tbr2*-EGFP construct were obtained from the Mutant Mouse Regional Resource Center. Animal experiments were approved by and performed in accordance with the Kawasaki Medical School Animal Experiment Protocol. The transplantation of neurally induced human ESCs was approved by and performed in accordance with the regulatory guidelines of the University of Brussels and validated by the ULB committee for animal welfare.

Ethylene glycol tetraacetic acid treatments

The ethylene glycol tetraacetic acid (EGTA) stock solution contained 200 mM EGTA (Sigma) dissolved in sterilized PBS. To prepare injection solutions, 1% first green (final concentration: 0.1%) and Cell Tracker Orange (CTO; final concentration: 50 μM; Lonza) were added to the stock solution. E14.5 mice were anesthetized by intraperitoneal administration of Somnopentyl (∼1.94 mg/mouse); then, an incision was made in the abdominal cavity, and the uterus

was exposed. The prepared injection solutions were injected into the embryonic brain ventricles with a micropipette connected to a mouth-controlled pipette system (Drummond Scientific) (∼1–2 μL/embryo; the injection volume was adjusted by the size of lateral ventricle at each developmental stage). The abdomen was sutured with nylon, and the animals were warmed and allowed to recover. After the animals were sacrificed, the brains were harvested and fixed with 4% paraformaldehyde (PFA) in 0.1 M phosphate buffer (at room temperature for 2 h or at 4°C overnight). After replacing the solution with 20% sucrose in 0.1 M phosphate buffer, the brains were sliced into 100-μm-thick sections using a Leica Microslicer (VT1000S). These slices were then immunostained with various antibodies and examined.

Transplantation into epithelial tissue using the calcium depletion method (Fig. 1A)

For the transplantation of dissociated brain cells, the telencephalons of E14.5 mice were harvested, the pia mater that had adhered to the periphery was peeled off, and the dorsal cortex was dissected out (in PBS on ice). The dorsal cortices were placed in a 2.0-mL tube, and 1 mL trypsin (0.25% from 2.5% solution; Gibco) was added. The tubes containing trypsin were incubated for 5 min at 37°C. Next, 1 mL of trypsin inhibitor (10 mg/mL; Roche) was added, and the dorsal cortices were dissociated via trituration by pipetting 10 times using a P1000 Pipetman. To remove clustered cells, the dissociated cell suspension was filtered through a cell strainer (40 μm; Falcon). After filtering, the collected cell suspension was centrifuged (1,000 rpm, 2 × 3 min), and after discarding the supernatant, 200 μL of PBS was added to create a suspension. The cell suspension was stained for 20 min with CTO or Cell Tracker Green (CTG; final concentration: 50 μM; Lonza). After rinsing twice at 1,000 rpm for 3 min, 200 μL of PBS was added, and the dissociated brain cell suspension was complete.

For the transplantation of neurally induced mouse ESCs, GFP-positive cells collected with fluorescence activated cell sorting (FACS) were centrifuged (1,000 rpm, 3 min), the supernatant was discarded, and 100 μL of Hank's balanced salt solution (HBSS) was added to prepare a cell suspension. CTO (final concentration: 50 μM) was added to this cell suspension, and the cells were stained for 20 min. The cells were rinsed with 1 mL HBSS and centrifuged (1,000 rpm, 3 min). The supernatant was discarded and 30 μL of HBSS was added to prepare a cell suspension. We noticed that the fluorescent signals of CTO or CTG became weaker after 2 weeks of labeling, although leaking of compounds from the stained cell was not observed.

The injection solution was prepared by adjusting the concentration of the cell suspension to 1.0×10^4 cells/μL with 1% Fast Green (Sigma; final concentration: 0.1%) and a 200-mM EGTA solution (final concentration: 20 mM). Injection into the embryonic brain ventricles and the subsequent specimen preparation were performed as described in the section "EGTA treatments."

Neural induction of ESCs

The induction of mouse ESCs to a cortical neuron fate was performed using an adherent monoculture system

described elsewhere [1,20]. The induction method of the H9 human ESC line that ubiquitously expresses GFP to a cortical neuron fate using an adherent monoculture system and the detailed characterization of induced neural cells using neural lineage markers were described previously [3]. GFP-expressing ESCs were differentiated into cortical-like cells for 24 days and then dissociated using Accutase (Invitrogen) for subsequent in utero transplantation via the transplantation into epithelial tissue using the calcium depletion (TETCaD) method.

FACS sorting

Neurally induced wild-type (MG1.19) [21] and *Sox1*-GFP mouse ESCs [22] in a culture dish were rinsed once with 1 mL HBSS ($1\times$, prepared by diluting $10\times$ with H_2O; Gibco), after which the cells were dissociated from the dish using Accutase (0.8 mL/dish; Invitrogen) with DNase (10,000 U/mL in 0.15 M NaCl; Sigma). HBSS (1.2 mL) was added to bring the total volume to 2 mL. The dissociated cells were centrifuged (1,000 rpm, 3 min), the supernatant was removed, and 4 mL of HBSS was added to prepare a suspension. At this time, the cells were counted and centrifuged again (1,000 rpm, 3 min). The final suspension was prepared at a concentration of 1.0×10^7 cells/mL or less. Using a fluorescent separator (FACSAria; Becton Dickinson), the prepared suspension was sorted into GFP-positive and GFP-negative cells (Supplementary Fig. S3B; Supplementary Data are available online at www.liebertpub.com/scd). The sorted cells were collected into a 15-mL tube containing DMEM/F12 (Gibco) culture medium. Harvesting in this way yielded between 5.0×10^5 and 3.0×10^6 cells. Some of the collected cells were plated on a plastic dish, cultured for 1 day, stained, and then examined. The remaining cells were later stained with CTO, used to prepare injection solutions, and then transplanted. Cells dissociated from the dorsal cortex of E14.5 *Tbr2*-EGFP mice were sorted in a similar manner.

Immunofluorescence

Immunofluorescence of brain slices was performed according to a previously described protocol [23]. The following primary antibodies were used: phospho-Histone H3 (PH3) (rabbit, 1:500; Upstate), Tuj1 (mouse, 1:500; Covance), VGluT2 (rabbit, 1:250) [24], GFP (chick, 1:500; Aves Labs or chick, 1:1,000; Abcam), Pax6 (rabbit, 1:500; Covance), Tbr2 (rabbit, 1:500; Abcam), CD24 (rat, 1:200; BD), MAP2 (rabbit, 1:250; Abcam), Ctip2 (rat, 1:200; Abcam), Satb2 (mouse, 1:200; Abcam), and all human nuclei (mouse, 1:1,000; Chemicon).

To examine the structure of the ventricular surface, the brain slices were first stained using phalloidin (Alexa Fluor 488 phalloidin conjugate; Invitrogen), which specifically binds to actin and DAPI (Molecular Probes). For this staining, the sections were incubated at 20°C for 2 h, rinsed three times with PBS, and then mounted.

Neurally induced *Sox1*-GFP ESCs used for transplantation were plated on a dish, incubated overnight, fixed for 10 min with 0.5% PFA, and stained. After incubating for 2 h using the primary antibodies described earlier (Pax6, Tuj1, and GFP antibodies, 1:1,000), the cells were incubated for 30 min with secondary antibodies, blocked, and examined. For immunostaining of brain tissue or slices, incubations were 5–6 days with primary antibodies and overnight with secondary antibodies.

All observations were conducted with confocal laser (Leica TCS SP2, Olympus FV-1000, and Carl Zeiss LSM510) and fluorescent microscopy (Carl Zeiss Axioplan2).

Time-lapse imaging of grafted cells

Cells dissociated from the dorsal cortex of E14.5 *Tbr2*-EGFP mice were sorted with FACS, and the GFP-positive populations were then grafted into the brains of E14.5 mice using the TETCaD method. The preparation of organotypic slice cultures is described elsewhere [12,25]. Briefly, the transplanted brains were harvested after 1 day, the telencephalon region was cut up, and the pia mater was removed. The dorsal cortex region was cut into sections of ∼300-μm thick with an ophthalmic knife and slices were prepared. The prepared slices were embedded in collagen (Cellmatrix Type I-A; Nitta Gelatin, Inc.) and incubated for ∼1 h at 37°C. After the collagen was sufficiently set, confocal laser microscopic observations were made (Olympus FV-1000).

Quantification

For the counting of grafted cells, ∼24 (100-μm thick) slices were prepared from each brain using a vibratome. A subset (8) of these slices were selected, stained with DAPI, and imaged with a confocal laser microscope. These images were analyzed with image analysis software (ImageJ, NIH, and Volocity Visualization; Perkin-Elmer) to produce reconstructed images that were used to count the number of grafted cells. The values were later multiplied threefold and recorded as the number of cells grafted into each brain. ImageJ software was used to measure the distance between the grafted cells and the apical surface.

Statistical analyses

To analyze the orientation of monopolar processes in the grafted tissue (Fig. 4B), we applied the methodology of directional statistics [26]. We examined whether a process was significantly oriented to a purely apical direction by evaluating the homogeneity of the angle by the value of cosθ. The result of the calculation showed that the monopolar processes of 7-day ESC-derived neural cells were significantly oriented to a purely apical direction ($P<0.01$), while the processes of 14-day cells were not.

For the process angle analysis of 7- and 14-day ESC-derived neural cells (Fig. 3D), we compared the cumulative distribution by using a Kolmogorov–Smirnov test and an Anderson–Darling test. We found that the difference in distributions between 7- and 14-day cells is significant using both tests ($P<0.01$ for both Kolmogorov–Smirnov test and Anderson–Darling test).

Results

EGTA injection into the ventricle of the developing cortex dramatically increases the efficiency of transplantation

In pilot studies performed to estimate transplantation efficiency, we found that neural progenitors dissociated from the developing mouse brain are infrequently

incorporated into the host brain tissue (see the section on Transplantation of cortical cells into developing brains treated with EGTA). We postulated that junctional complexes at the apical surface prevent the incorporation of the grafted cells into the developing brain by acting as a barrier of epithelial tissue. We therefore explored the possibility that a reduced calcium concentration might dissociate the apical junctions because adherens junctions are mainly composed of homo-typically bound cadherin proteins, which are dependent on calcium concentration [27]. To reduce calcium concentrations, we added an EGTA solution, a specific chelator of calcium ions that has been reported to dissociate adherens junctions in cultured epithelial cells [28,29]. We injected various concentrations (1–150 mM) of EGTA into the ventricles of embryonic (E14.5) mouse cortex through in utero surgery and observed the apical surface structure 2 h after the operation. The honeycomb pattern of actin organization that covers the entire apical surface was recognizable with EGTA injection concentrations up to 20 mM (Fig. 1B), indicating that apical surface junctions remain intact under these concentrations of EGTA. Remarkably, the disruption of actin organization at the apical surface could be recognized in 25% of embryos injected with 30 mM EGTA and in 69% of embryos injected with 50 mM or more (Fig. 1B), indicating that apical junctions in the epithelial tissue of the developing brain are dissociated in the presence of higher doses of EGTA.

We further assessed the concentration of EGTA that could be injected without adverse effects on normal brain development by applying 0, 20, 30, or 50 mM EGTA solution to the ventricle of the developing mouse brain. It has been shown that mitosis in neural progenitors takes place at the apical surface, at the basal region of the ventricular zone (VZ), and in the SVZ [13–15]. We found that PH3-positive mitotic cells were significantly decreased at the apical surface and increased at the non-apical region in embryos injected with 30 and 50 mM, but not with 20 mM, of EGTA [Fig. 1C, absolute numbers of apical and non-apical mitotic cells per 100 μm of ventricular surface; 11.1 ± 1.3 (EGTA: 0 mM), 13.4 ± 0.8 (20 mM) (not significant, n.s.; t-test) and 5.7 ± 0.7 (0 mM), 6.0 ± 1.0 (20 mM) (n.s., t-test), respectively. Error values are SEM]. The gross organization of Tuj1-positive postmitotic neurons was similar in all conditions (Fig. 1C), suggesting that the

higher concentrations of EGTA solution largely affect the tissue structure of the VZ rather than neuronal organization in the cortical layers. We next examined the anatomical profiles of postnatal brains injected with EGTA at the embryonic stage. Aberrant hydrocephalic cortices began to occur with 30 mM EGTA, and the likelihood of occurrence increased when 50 mM was injected (Fig. 1D). In contrast, the gross brain structure was intact from postnatal day (P)0 up to P58 in 93% of the 20-mM-injected brains (Fig. 1D and Supplementary Fig. S1A). We confirmed successful injection of EGTA into the cortical ventricles based on the remaining fluorescent signal of the vital dye injected with the EGTA solution (Supplementary Fig. S1B). We measured the brain weight, thickness of the dorsal cortex, and the length of the ventricular and cortical surfaces of the P10 mouse brain, verifying that there were no significant changes between 0 and 20 mM EGTA [brain weight, 7.9 ± 0.1 g (0 mM, $n = 11$) and 7.6 ± 0.2 g (20 mM, $n = 12$) (n.s., t-test); thickness of dorsal cortex, 883 ± 38 μm (0 mM, $n = 14$) and 932 ± 32 μm (20 mM, $n = 16$) (n.s., t-test); length of ventricular surface, $1,090 \pm 40$ μm (0 mM, $n = 15$) and $1,006 \pm 49$ μm (20 mM, $n = 16$) (n.s., t-test); length of cortical surface, $1,271 \pm 6.6$ μm (0 mM, $n = 15$) and $1,254 \pm 8.8$ μm (20 mM, $n = 16$) (n.s., t-test). Error values are SEM]. We further sought to determine whether the presence of EGTA induces lesions in the layered structure of the postnatal mouse cortex using the immuno-reactivity of a VGluT2 antibody [24]. Following the injection of 20 mM EGTA, the cortical layer architecture appeared identical to the control (0 mM EGTA) at both P0 and P58 (Fig. 1D). This observation was further verified by immunostaining using specific markers of deeper and upper layer neurons (Ctip2 and Satb2, respectively; Supplementary Fig. S2A) and by birthdating analysis by EdU labeling of newborn neurons after the EGTA treatment (Supplementary Fig. S2B). Finally, we examined the ependymal layer surrounding the lateral ventricle at P10 and found that actin organization at the ventricular surface and localization of CD24, a marker of ependymal cells [30], were intact after the injection of 20 mM EGTA (Supplementary Fig. S2C). These results confirm that injection of 20 mM EGTA induces little damage, if any, to the structure of embryonic and postnatal mouse brains.

FIG. 1. Effect of ethylene glycol tetraacetic acid (EGTA) injection into the lateral ventricle of the developing brain. **(A)** The design of the experiments performed in this study. We performed in utero transplantation with EGTA using neural cells dissociated from developing mouse brains or derived from mouse and human (not shown here) embryonic stem cells (ESCs). Grafted cells and the host brain tissues were characterized. **(B)** EGTA dissociates apical junctions in the neuroepithelium in a concentration-dependent manner. **(a)** Low-magnification view of the developing mouse cortex (E14.5). **(b)** Effects of EGTA on the actin organization (*green*) of the apical surface assessed from the lateral (*left columns*) and the apical sides (*right columns*). *Green*, actin; *white*, DNA. **(C)** Excessive doses of EGTA impair the positioning of mitotic cells in the neuro-epithelium. The position of apical mitotic cells [phospho-Histone H3 (PH3)-positive cells, *white*] was examined 1 day after the injection of EGTA into the E14.5 mouse brain. The population of mitotic cells at the apical surface is essentially the same when 0 and 20 mM EGTA are injected **(a, b, and e)**, while the number of ectopic, non-apical mitotic cells is increased at EGTA concentrations of 30 and 50 mM **(c, d, and e)**. Note that the gross organization of the postmitotic neurons (Tuj1-positive, *red*) is nearly intact when up to 50 mM EGTA is injected **(a–d; *right panels*)**. Scale bar in **(a)** = 50 μm. *$P < 0.05$, t-test. Error bars; SEM. **(D)** The gross brain structures of postnatal (P) mice remain intact after the injection of 20 mM EGTA. **(a)** Ratio of normal brains at various postnatal stages after the injection of 0, 20, 30, or 50 mM EGTA at E14.5. Postnatal stages were categorized as 0 to 5, 6 to 10, and 11 to 58 days after birth. *n*, the number of animals tested in each category. **(b–e)** Brains (*left panels*) and cortical layers (*right panels*) at P0 **(b, d)** and P58 **(c, e)** after injection of 0 **(b, c)** or 20 **(d, e)** mM EGTA at E14.5. Cortical layers were visualized through immunostaining with a VGluT2 antibody [24]. Scale bars for *left panels* = 1 mm, for *right panels* = 200 μm. Color images available online at www.liebertpub.com/scd
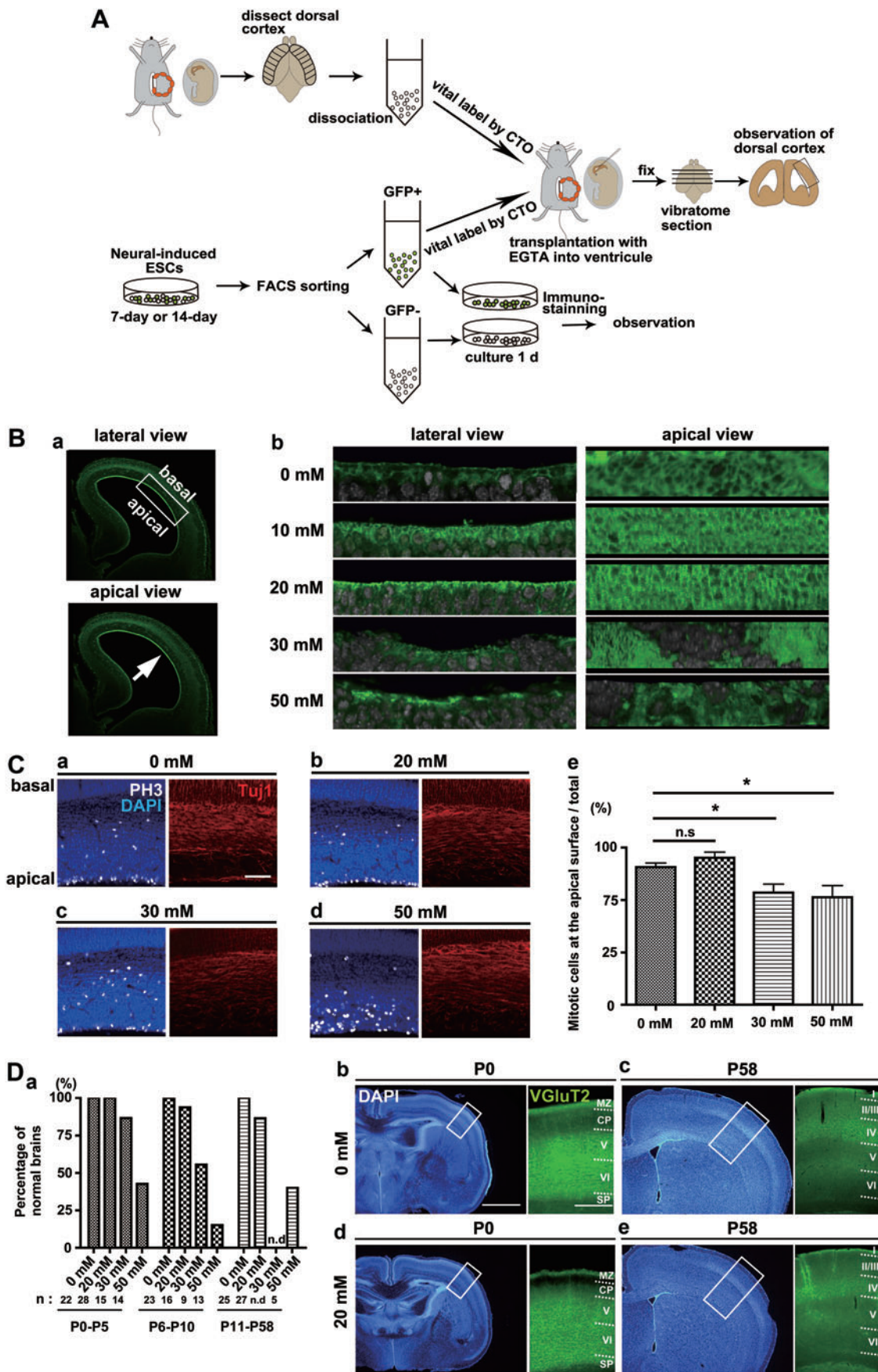
*Transplantation of cortical cells into developing
brains treated with EGTA*

To determine whether the EGTA treatment increased the transplantation efficiency of neural cells into the epithelial tissue of the developing cortex, we injected mouse cortical cells dissociated from the dorsal cortex at E14.5 as grafting cells. These cells included both neural progenitors and neurons. The dissociated cortical cells were labeled with fluorescent vital dye and injected into the ventricle of an E14.5 mouse along with the EGTA solution (see Fig. 1A for the procedure). Surprisingly, the number of grafted cortical cells in the dorsal cortex of the host embryos significantly increased when 20 or 30 mM EGTA was applied ($\sim$100 or 300 times, respectively, compared with 0 mM; Fig. 2A). A reduced number of grafted cells in the 50-mM EGTA condition might reflect an impairment of cell survival due to the excessive dose of EGTA (Fig. 2A). Taken together, our results support the idea that the presence of a moderate concentration of EGTA increases the efficiency of transplantation, likely through the partial dissociation of adherens junctions in the epithelial tissue due to the chelation of calcium (Fig. 1B). It is surprising that the number of grafted cells was increased dramatically by treatment with 20 mM EGTA without showing disruptions in apical adherens junctions and brain tissue architecture (Fig. 1 and Supplementary Figs. S1 and S2). Possibly, self-organization of apical junctions might take place soon after the EGTA treatment. Moreover, grafted cells dispersed in the host brain, allowing us to assess their morphology with single-cell resolution. Hereafter, we refer to these experimental procedures as the "TETCaD (transplantation to epithelial tissue with calcium depletion)" method. In subsequent experiments, to characterize the grafted cortical cells, we used a 20-mM concentration of EGTA for injection into the ventricle of the E14.5 cortex to avoid the adverse effects to the host tissue and grafted cells caused by excessive doses of EGTA.

Endogenous neurons generated from neural progenitors in the dorsal cortex migrate toward the cortical plate during development (radial migration) [31]. We tested whether neural cells grafted using the TETCaD method also migrate basally within the host tissue. The distance of grafted cortical cells from the apical surface was quantified in host mice that were sacrificed 1–3 days after transplantation (at E15.5 or E17.5, respectively). A large number of grafted cells were identified in regions away from the apical surface 3 days after transplantation (Fig. 2B). This result indicates that grafted cells migrate toward the pial surface in the host brain. To further confirm this result, we attempted to observe the migration of grafted cells directly through time-lapse imaging analysis using an organotypic slice culture of the developing brain [10]. Cortical cells dissociated from embryos of *Tbr2*-EGFP mice allow us to identify newly born cortical neurons by the fluorescence of GFP driven by the *Tbr2* promoter [32]. GFP-positive grafted cells exhibited neuronal migration-like movement in an apical to basal direction, following a trajectory perpendicular to the ventricular surface (Fig. 2C and Supplementary Movies S1 and S2). Consistent with in vivo neuronal migration in the dorsal cortex [31], migrating grafted cells extended their leading processes in the direction of their heading orientation (Fig. 2C). Grafted cells in the dorsal cortex showed a neural morphology in postnatal stages with extensions of axon- and dendrite-like neurites (Fig. 2D). Dendritic marker MAP2-positive long neurites, which resemble the apical dendrite of a pyramidal cell, were extended toward the pial surface in all cases ($n = 10$) (Fig. 2D). Taken together, these results demonstrate that cortical cells grafted through the TETCaD method can exhibit neuronal migration and differentiate into mature neurons in the dorsal cortex in vivo.

*Grafted cortical cells induced from mouse
ESCs show the extension of processes
along the apico-basal epithelial polarity*

To address the question of whether and how cortical cells induced from pluripotent stem cells acquire cytoarchitecture in response to spatial information from the host tissue, we designed experiments to graft ESC-derived cortical cells [1,20] into the developing cortex. *Sox1*-GFP mouse ESCs, which allow us to distinguish differentiating cells within the neuronal lineage based on GFP expression driven by the *Sox1* promoter [22], were subjected to neural induction for either 7 or 14 days (Supplementary Fig. S3A), and the GFP-positive population was selectively collected by cell sorting

FIG. 2. Transplantation of cortical cells into the developing mouse cortex using the transplantation into epithelial tissue using the calcium-depletion (TETCaD) method. **(A)** Transplantation efficiency is increased with EGTA treatment. Cortical cells were prepared from the dorsal cortex of E14.5 mice and then injected along with 0 **(a)** or 20 mM **(b)** EGTA solution into the lateral ventricle of an E14.5 mouse in utero. **(a, b)** Grafted cells [*green*, Cell Tracker Green (CTG) positive] in the developing cortex are observed 1 day after transplantation (*arrowheads*). Scale bar = 100 μm. **(c)** Number of grafted cortical cells per brain. For the details of quantification, see "Materials and Methods" section. *$P < 0.05$, *t*-test. **(B)** The position of grafted cortical cells shifts basally in the cortex following transplantation. **(a, b)** Cells (*green*, CTG positive, *arrowheads*) in the developing cortex 1 **(a)** or 3 days **(b)** after transplantation. *Straight lines* indicate the distance of grafted cells from the apical surface. Scale bar = 20 μm. **(c)** Quantification of the position of cells from the apical surface 1 ($n = 136$) or 3 days ($n = 109$) after transplantation. ***$P < 0.001$, *t*-test. **(C)** Grafted *Tbr2*-EGFP-positive cortical cells (*green*) migrate basally, extending their leading process. **(a)** An organotypic brain slice prepared 1 day after transplantation of dorsal cortical cells [*red*, Cell Tracker Orange (CTO) positive] of E14.5 *Tbr2*-EGFP mice. Scale bar = 200 μm. **(b, c)** Time-lapse sequence of the migrating cells (*arrows*) depicted in **(a)**. *Arrowheads*, leading processes. Scale bar = 20 μm. **(D)** Grafted cortical cells in the postnatal brain. **(a)** Low-magnification view of P5 mouse cortex fixed 10 days after transplantation at E14.5. *Red*, grafted cortical cells labeled with CTO; *white*, DNA labeled with DAPI. Scale bar = 200 μm. **(b)** High-magnification view of the grafted cells highlighted in **(a)**. *Arrowhead*, axon-like neurite; *arrow*, dendrite-like neurite. Note that the vital dye (CTO) remains and does not leak from the grafted cell at 10 days after transplantation. Scale bar = 20 μm. **(c)** A grafted cell extending an MAP2-positive dendrite toward the pial surface (*arrow*). *Red*, grafted cortical cells; *green*, MAP2. Scale bar = 20 μm. *White* and *yellow dots*: the apical surface and the basal pial surface, respectively. Error bars in the graphs: SEM. Color images available online at www.liebertpub.com/scd
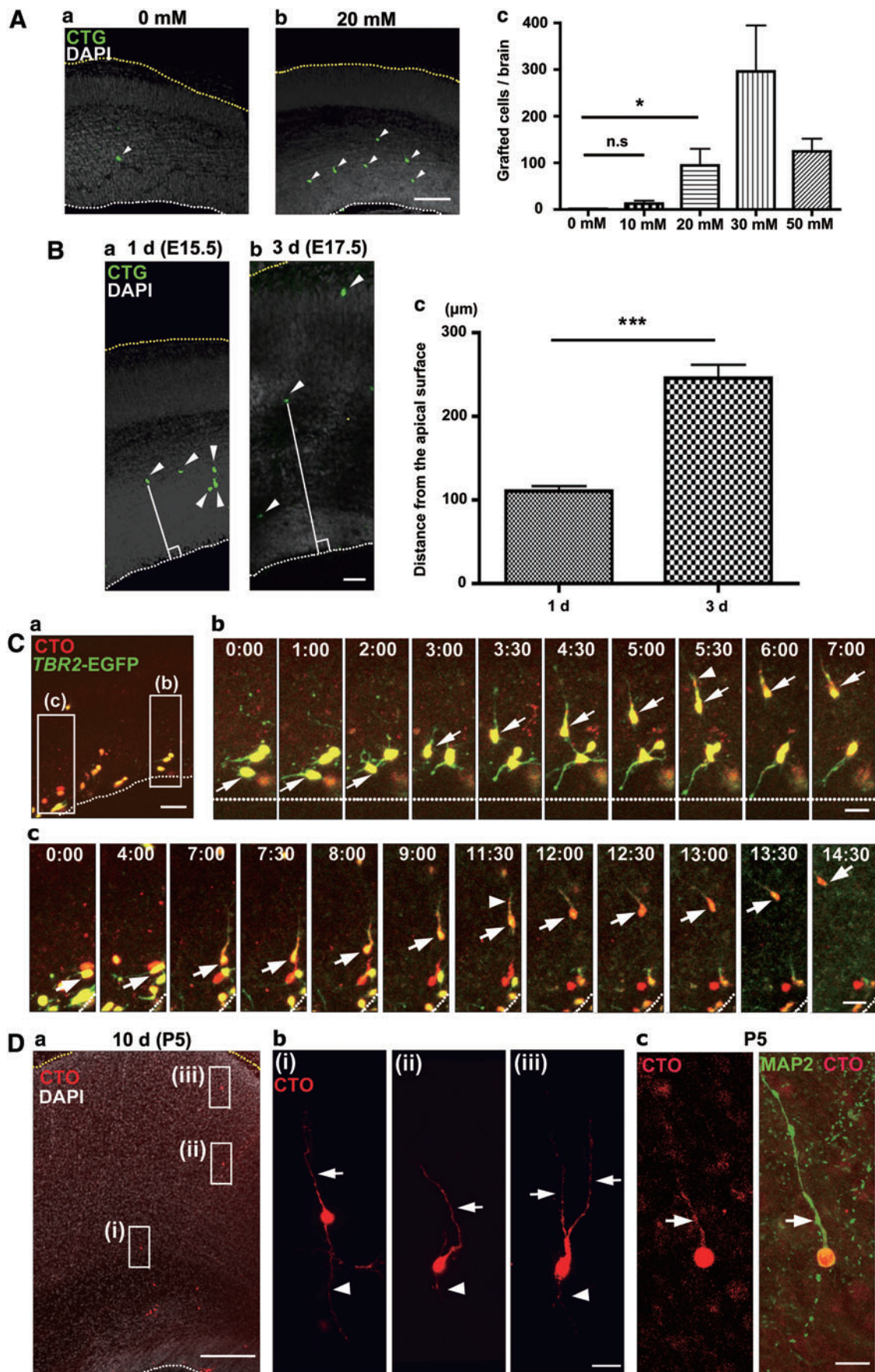
(Supplementary Fig. S3B). Among the GFP-positive population, a minor population (3.0%) was composed of Oct4-positive undifferentiated cells. The fate of the collected cells was examined using Tuj1 and Pax6 antibodies, markers of postmitotic neurons and self-renewing progenitors in the dorsal cortex, respectively (Fig. 3A and Supplementary Fig. S3C). Tuj1-positive cells increased at 14 days (43.8%) of neural induction compared with 7 days (9.6%), confirming that neural differentiation took place adequately.

We then grafted the *Sox1*-GFP-positive population into the embryonic mouse cortex using the TETCaD method. ESC-derived cells were incorporated into the tissue effi-

ciently (Fig. 3B), similar to the dissociated cortical cells. We found that the number of grafted ESC-derived cells was highly dependent on the development stage of the host embryo; more cells were incorporated on E12.5 compared with E14.5, while much fewer cells were incorporated on E17.5 (Fig. 3B). Without EGTA, <1 ESC-derived cell per brain (on average) was incorporated at E14.5 (Fig. 3B). Remarkably, grafted GFP-positive cells extended processes in the host brain tissue (Fig. 3C). We quantified the orientation of the processes extended from the grafted *Sox1*-GFP-positive cells relative to the apico-basal epithelial axis (Fig. 3D). Notably, there were strong tendencies in the orientation
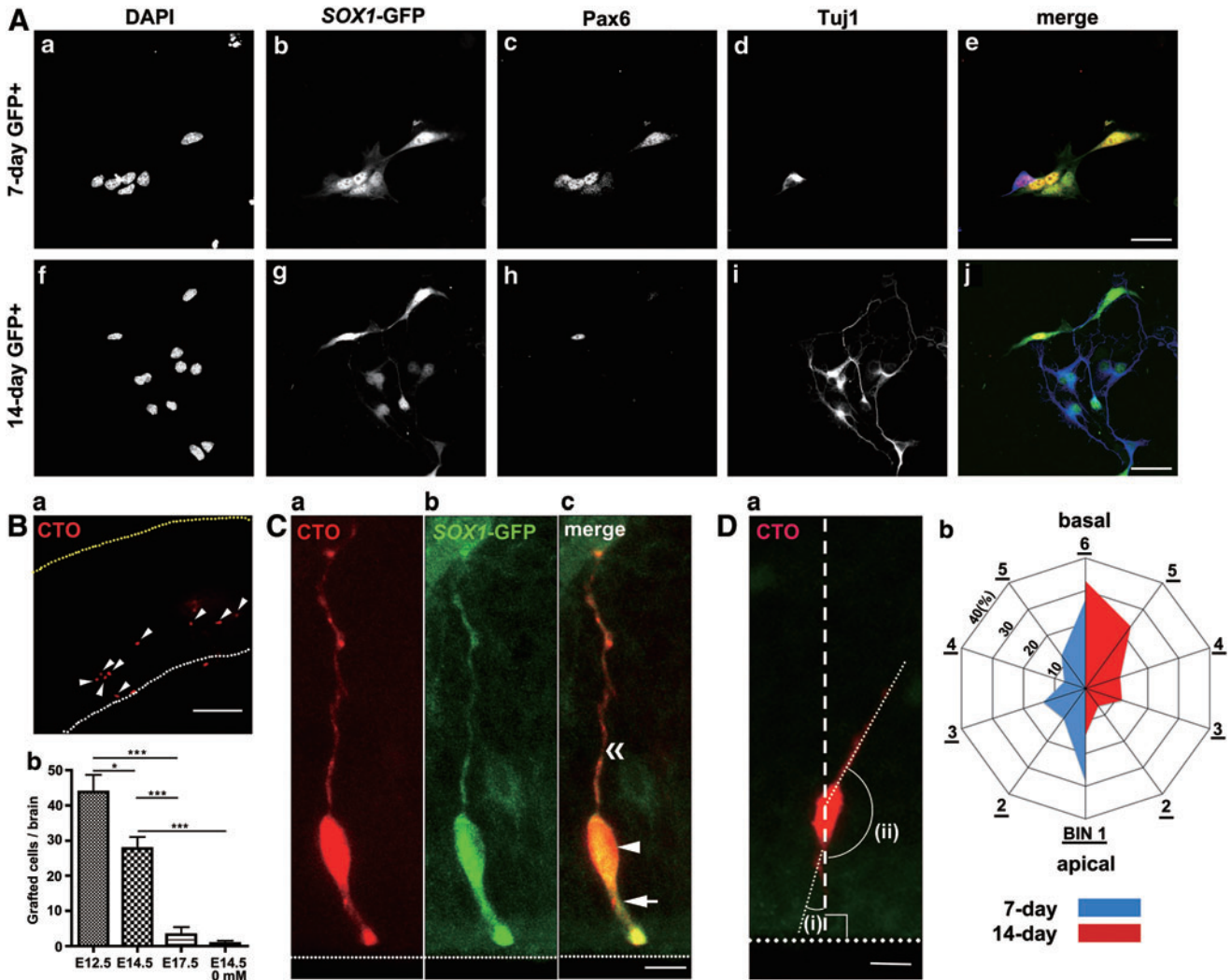

FIG. 3. Transplantation of mouse-ESC-derived cortical cells into the developing mouse cortex using the TETCaD method. **(A)** Neural induction of a *Sox1*-GFP mouse ESC line [22] to a cortical cell fate. The time course of neural induction was 7 **(a–e)** or 14 days **(f–j)**. DNA **(a, f)**, *Sox1*-GFP **(b, g** and **e, j;** *green*), Pax6 **(c, h** and **e, j;** *red*), and Tuj1 **(d, i** and **e, j;** *blue*). Scale bars = 30 μm. **(B-a)** Mouse-ESC-derived cells grafted to the developing mouse cortex (*red*, CTO positive, *arrowheads*) using the TETCaD method. **(b)** Number of grafted ESC-derived cells per brain. Transplantations and cell counting were performed using E12.5, E14.5, and E17.5 mice brains with 20 mM EGTA, and E14.5 without EGTA. The time course of neural induction was 10 days. *$P < 0.05$ and ***$P < 0.001$, *t*-test. Error bars: SEM. **(C)** Grafted mouse-ESC-derived cells extend processes in the dorsal cortex. **(a–c)** A grafted *Sox1*-GFP-positive cell (*arrowhead*) with apically (*arrow*) and basally (*double arrowhead*) directed processes is recognized with CTO **(a)** and the expression of *Sox1*-GFP **(b)**. Scale bar = 5 μm. **(D)** Measurement of the angle of processes relative to the apico-basal axis (*dashed line*). **(a)** The angles of processes oriented in the apical (i) and basal (ii) directions were measured as represented. Scale bar = 5 μm. **(b)** Quantified angle of processes extended from grafted cells. The sector is subdivided into bins of 30°, numbered 1, 2, and so on, from the purely apical direction. Neural induction was 7 (*blue*, $n = 88$) or 14 days (*red*, $n = 316$). *White* and *yellow dots*: the apical surface and the basal pial surface, respectively. Color images available online at www.liebertpub.com/scd

of extended processes depending on the duration of neural induction. When neural induction took place for 7 days, processes tended to be extended in both the apical and basal directions [bin 1 (0°–30°, 28%) and 6 (150°–180°, 27%), respectively, in Fig. 3D]. For cells induced for 14 days, the population of basally oriented processes dominated [bin 5 plus 6 (120°–180°, 56%) in Fig. 3D]. The distribution difference between 7- and 14-day cells was statistically significant ($P < 0.01$, for both Kolmogorov–Smirnov test and Anderson–Darling test). These results demonstrate that ESC-derived cortical cells grafted into tissue have the

ability to extend processes along the apico-basal epithelial polarity. Further, the orientation of the processes depends on the duration of neural induction (ie, 7 or 14 days).

To further understand the correlation between process formation and the intrinsic cell fate of the grafted cells, we attempted to more precisely distinguish between self-renewing neural progenitors (Pax6-positive) and postmitotic neurons (Tuj1-positive) within the population of GFP-positive grafted cells. We also performed immunostaining for glial cells or intermediate neural progenitors (GFAP- or Tbr2-positive cells, respectively). Of the grafted cells, 3.9% and
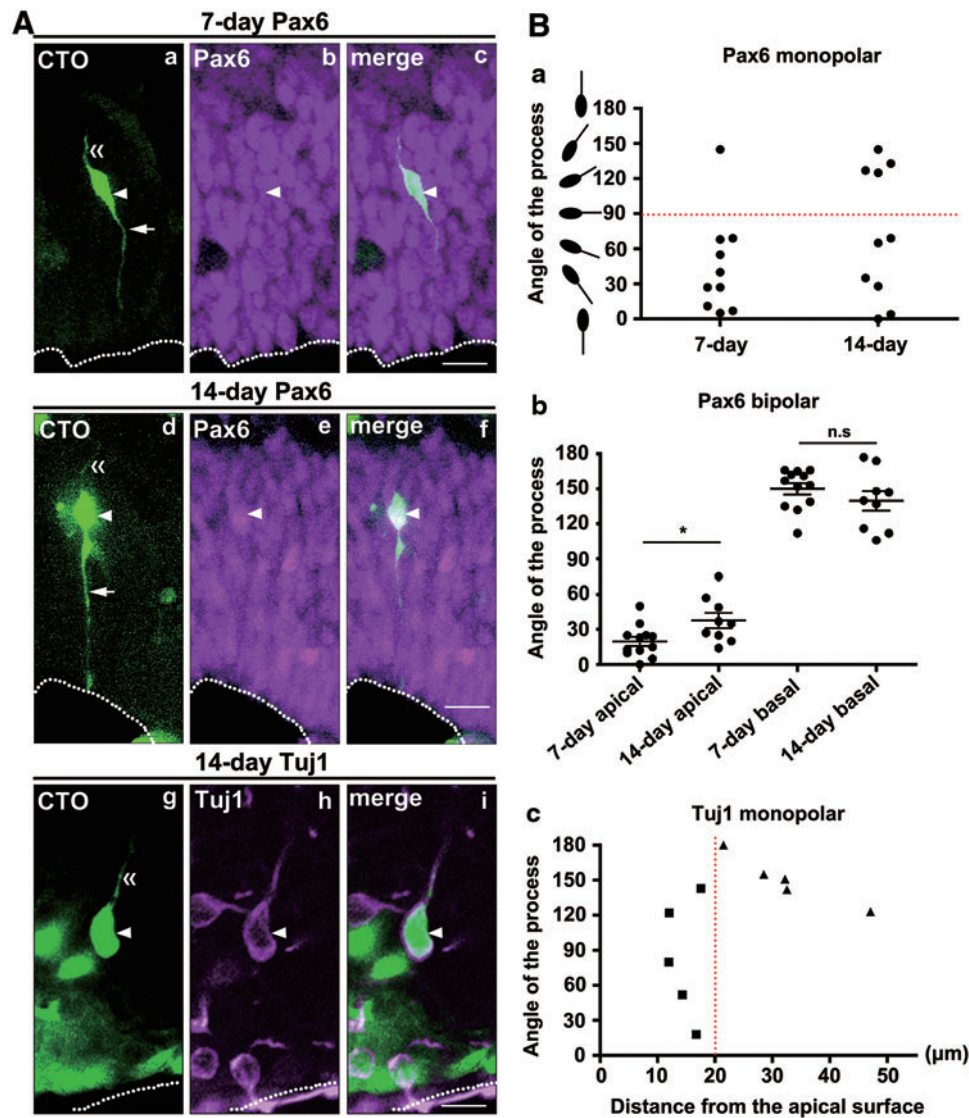

FIG. 4. Mode of process extension is dependent on the apico-basal epithelial polarity of the host tissue and the differentiation state of the grafted cells. **(A)** ESC-derived cortical cells (*green*, CTO positive) grafted into the dorsal cortex exhibit fates of dorsal cortical progenitors **(a–f,** Pax6 positive) or postmitotic neurons **(g–i,** Tuj1 positive). Grafted cells (*arrowheads*) extending apical and basal processes (*arrows* and *double arrowheads*, respectively). Neural induction was 7 **(a–c)** or 14 days **(d–i)**. *Magenta*: Pax6 **(b, c, e,** and **f)** or Tuj1 **(h, i)**. Confocal images are stacked in **(a, d, e,** and **g)**. *White dots*: apical surface. Scale bars = 10 μm. **(B)** Measurements of process orientations. **(a)** Orientation of monopolar processes extended from Pax6-positive grafted cells after 7 ($n = 10$) or 14 ($n = 10$) days of neural induction. *Red dashed line*: the border of apical and basal orientations (90°). **(b)** Orientation of bipolar processes extended from Pax6-positive grafted cells after 7 ($n = 12$) or 14 ($n = 9$) days of neural induction. The apically and basally oriented processes of each cell are displayed separately. *$P < 0.05$, *t*-test. **(c)** Orientation of monopolar processes extended from Tuj1-positive grafted cells after 14 days of neural induction ($n = 10$). *Red dashed line* indicates 20 μm from the apical surface. Angles were measured from the purely apical direction (Fig. 3D). Error bars in the graphs represent the SEM. Color images available online at www.liebertpub.com/scd

3.4% were positive for Tbr2 and GFAP, respectively. We could not find significant correlations between either marker and a particular cell shape. For Pax6-positive grafted cells, we found both monopolar and bipolar morphologies, mostly in the VZ, without noting differences in the positions relative to the apical surface (Fig. 4A and Supplementary Fig. S4). Approximately half of grafted cells showed a bipolar morphology, which resembled endogenous Pax6-positive apical progenitors, in both the 7-day (55%) and 14-day (47%) neural induction cases. For monopolar cells, we found that processes of the 7-day neural induction cells were significantly oriented toward the apical side ($P < 0.01$, based on the directional statistic analysis), while this tendency was not observed in the 14-day cases (n.s., t-test) (Fig. 4B). For bipolar cells, we analyzed the orientation of apically and basally directed processes and found that grafted cells extended processes in a more apical direction ($19.8° \pm 4.0°$) after 7 days of neural induction compared with 14 days ($37.7° \pm 6.5°$) (Fig. 4B). We did not find significant differences in the basally oriented processes of neural induction cases between 7 and 14 days (Fig. 4B). These results indicate that, in both monopolar and bipolar Pax6-positive grafted cells, the ability to extend apically oriented processes appears to be stronger with a shorter period of neural induction (7 days) than with a longer period (14 days), possibly reflecting a difference in the differentiation state of the Pax6-positive self-renewing progenitors.

Next, we analyzed the morphology of Tuj1-positive grafted cells. These cells have already differentiated into neurons and lost their stemness. Most of the Tuj1-positive grafted cells (77%) exhibited a monopolar morphology (Fig. 4A). Notably, grafted cells close to the apical surface ($< 20 \mu m$) extended processes in nonspecific orientations ($83.0° \pm 22.7°$), while basally oriented processes ($150.2° \pm 9.3°$) were significantly dominant ($P < 0.05$, t-test) in cells located more than $20 \mu m$ away from the apical surface (Fig. 4B). This result implies that cellular position in the apico-basal axis in the host tissue affects the orientation of processes extended from postmitotic neurons. Taken together, these results document that the mechanism of process extension in both neural progenitors and neurons induced from ESCs is not stochastic but likely depends on the extrinsic apico-basal epithelial polarity, as well as on the intrinsic differentiation state of the grafted cells.

Robust incorporation of cortical neural progenitors induced from human ESCs into the developing mouse brain using the TETCaD method

We next examined whether the TETCaD method is applicable to human cortical progenitors, which can be obtained efficiently from human ESCs or iPSCs [2,3]. At 24 days after the initiation of cortical differentiation from GFP-expressing human ESCs, the cells in the culture dish can be immunostained for the cortical progenitor marker PAX6 and the differentiated neuron marker TUJ1 (Supplementary Fig. S5A). A majority of the cells (86.8%) were PAX6$^+$/TUJ1$^-$, and only a minor population (3.9%) was PAX6$^-$/TUJ1$^+$ (Supplementary Fig. S5B). GFP-expressing human ESCs were injected into the cortical ventricle of a mouse embryo at E14.5 using the TETCaD method. The grafted human cells successfully integrated with high efficiency and remained in the developing mouse cortex (Fig. 5A and Supplementary Fig. S6). Importantly, in the absence of EGTA coinjection, < 1 cell per brain was integrated into the host mouse brain (data not shown). Host mice were sacrificed after 1 day (E15.5), 3 days (E17.5), or 6 days (P0) to examine the identity, morphology, and distribution of the transplanted cells within the host cortex. The human-ESC-derived cells were incorporated exclusively in the VZ at E15.5 but they spread in the cortical plate as cortical development proceeded (Fig. 5A). Notably, in contrast to cortical cells dissociated from mouse embryos, grafted human-ESC-derived cells stayed in the VZ for a longer period of time before migrating into the cortical plate (Fig. 2B). We found that PAX6-positive cells tended to be clustered in the VZ (Fig. 5B), while single cells isolated from the clusters displayed an apico-basally elongated morphology (Fig. 5C), similar to endogenous apical progenitors in the developing mouse and human cortices [17]. As single cells displayed apico-basally polarized cytoarchitecture, human-ESC-derived cortical progenitors are capable of establishing polarity by adapting to the extrinsic in vivo environment of the developing mouse cortex.

TUJ1-positive grafted cells displayed a polarized morphology with a long basally directed process (Fig. 5D). On the subsequent days, those cells were consistently found at more basal positions toward the cortical plate, thus mimicking radial migration (Fig. 5A). Transplanted NESTIN (a

FIG. 5. Transplantation of human-ESC-derived cortical cells into the developing mouse cortex using the TETCaD method. **(A)** Grafted GFP-expressing human-ESC-derived cells (24 days of differentiation, *green*) in E15.5 **(a)**, E17.5 **(b)**, and P0 **(c)** mouse cortex counterstained with hoechst33342 (*blue*). **(B, C)** Grafted human-ESC-derived cells 1 day after grafting (E15.5) labeled with the PAX6 antibody (*magenta*). **(B)** PAX6-positive donor cells (*arrowheads*) tend to be clustered in the host ventricular zone (VZ) without showing apparent apico-basal polarity. **(C)** A single GFP-expressing PAX6-positive donor cell (*filled arrowhead*) extends apical (*arrow*) and basal (*double arrowheads*) processes in the minority of cases. The other cell is negative for PAX6 (*open arrowhead*). **(D)** A TUJ1 (*magenta*)–positive grafted cell (*arrowhead*) displays immature neuron-like morphology. **(E)** Grafted cells in the cortical plate of a P0 host brain show bipolar morphology with apico-basally elongated processes **(a)**. Basally elongated processes are closely associated with the Nestin-positive radial fibers of the host cortex (**b**; *magenta*, *arrowhead*). Note that the grafted cell (*green*) is NESTIN negative, indicating that the cell has already differentiated. **(F)** Grafted human-ESC-derived cortical cells in the P7 mouse somatosensory cortex. Human cells were immunostained by a GFP antibody (*green*) and counterstained with hoechst33342 (*blue*). **(a)** GFP-positive human cells are scattered throughout the cortical layers. **(b)** Grafted human cells show apico-basally polarized morphology similar to that observed in endogenous mouse immature cortical neurons. **(c)** A few cells have a pyramidal morphology, in which there is a single long neurite (*arrowhead*) and multiple shorter neuritis. Scale bars = $100 \mu m$ **(A, F-a)**, $10 \mu m$ **(B–D)**, and $50 \mu m$ **(E, F-b** and **c)**. All *panels* are depicted with a basal (*yellow dots*)-above, apical (*white dots*)-below orientation. Color images available online at www.liebertpub.com/scd

marker of neural progenitors and radial glial cells)–negative differentiated cells in P0 cortical plates displayed bipolar elongated shapes, with processes that were closely associated with the Nestin-positive radial glial fibers of the host mouse cortex, similar to radially migrating endogenous neurons [33] (Fig. 5E). We further examined whether transplanted human-ESC-derived cells were maintained in the host mouse brain for a longer duration. When human-ESC-derived cells (32 days of differentiation) were transplanted into E14.5 mouse cortex, grafted cells were detected in the host cortical tissue at P7 (Fig. 5F), but were not extensively detected at P28 (data not shown). This result suggests that grafted human-ESC-derived cortical cells have a limited survival period in the mouse cortex after transplantation. Human cells were distributed in all cortical layers of host mice at P7 (Fig. 5F). Those cells exhibited
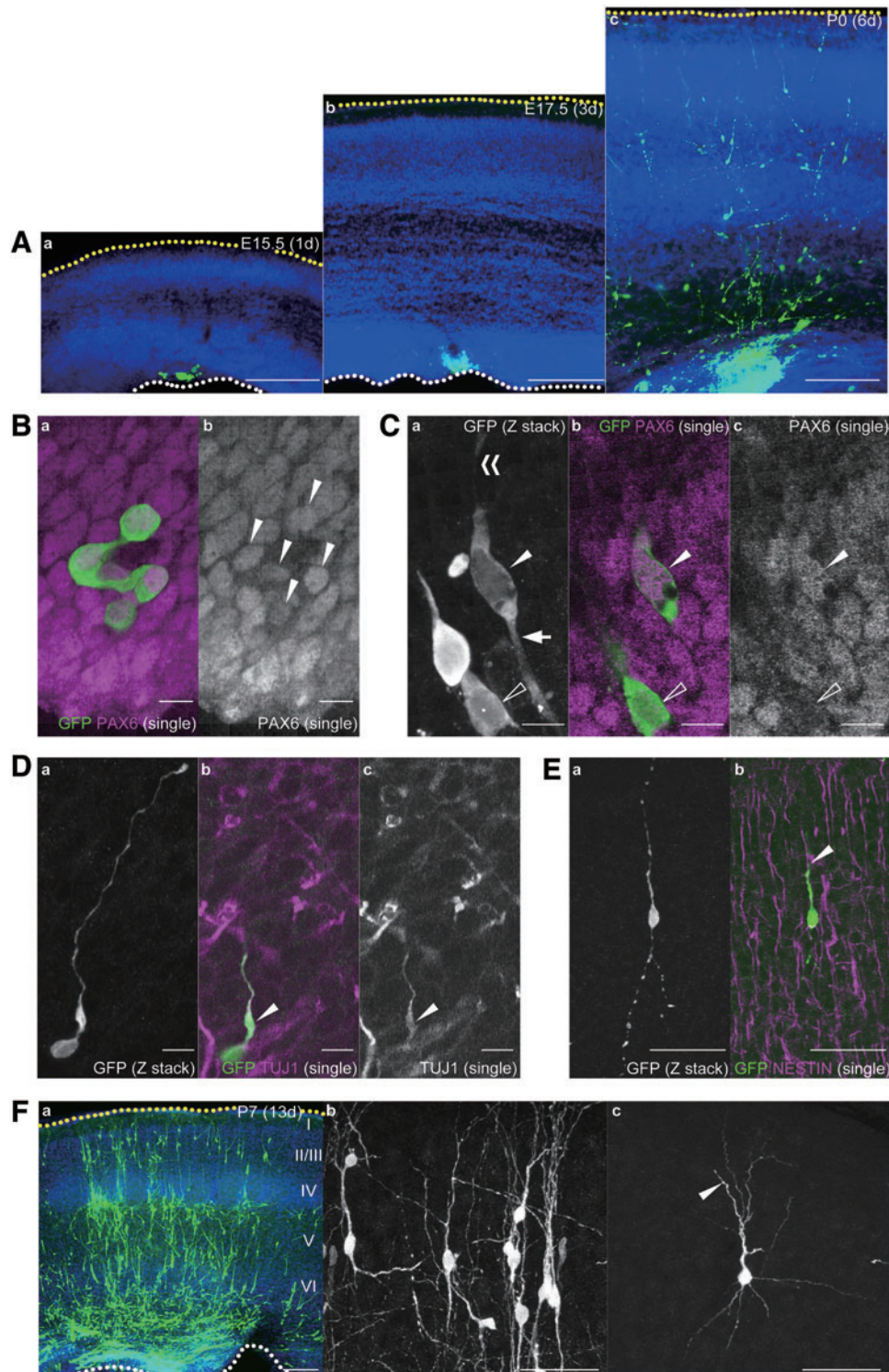
either an apico-basally oriented morphology, which is observed in migrating mouse cortical neurons, or a pyramidal morphology, which is characterized by a single longest neurite pointing toward the pial surface and multiple thinner neurites (Fig. 5F). Our results document that human-ESC-derived cortical neurons exhibit multiple features of radially migrating neurons in the mouse cortex. Human cortical cells thus integrated successfully into the host embryonic cortex, displaying appropriate morphology in accordance with the extrinsic apico-basal polarity and transitioning toward the acquisition of pyramidal neuron characteristics.

Discussion

In this report, we established a novel transplantation system, the TETCaD method, which enables the robust introduction of cortical cells dissociated from tissue or induced from mouse and human ESCs into the developing mouse cortex and permits us to observe their cellular morphology with single-cell resolution. Only a few neural cells of any source we tested were incorporated without using the TETCaD method (Figs. 2A and 3B). Notably, the number of incorporated cells without TETCaD was much lower compared to past works of transplantation to the developing cortex [34–36]. Although there are a number of possibilities to explain the differences between studies, we believe that the method of injection is one of the pivotal reasons. In previous works, glass micropipettes connected to a hydraulic microdrive [37] or Hamilton syringes [36] were used for injection. Here, we used a mouth-controlled pipette system, which enables more accurate and fine manipulations [38], resulting in less leakage throughout the injection. Using this system, we are able to avoid the unexpected incorporation of donor cells into the tissue parenchyma upon penetration of the micropipette. Moreover, we visualized the injection solution using Fast Green to immediately see whether there was a leak from the tip of the micropipette. Although we do not exclude other possibilities that may explain the differences in the incorporation rates, the technical point indicated above needs to be considered.

A predominant advantage of the transplantation approach in studying brain development is that it offers a way of dissecting neural cell behaviors to determine whether they are intrinsic or extrinsic [39]. Taking advantage of this attribute, we examined the mechanism of process formation in neurally induced mouse ESCs and found that the extension of cellular processes is dependent on the extrinsic apico-basal epithelial polarity of the host tissue, as well as on the intrinsic differentiation state of the grafted cells. The role of intrinsic and extrinsic factors in determining the behavior of neural progenitors has attracted researchers' interest [40]. As described in the ''Introduction'' section, the entire neurogenic process, from an undifferentiated stem cell to a terminally differentiated cortical neuron, can be tracked within the defined conditions of a culture dish [1,3,4], indicating that intrinsic pathways are sufficient for the overall differentiation of cortical neurons. Interestingly, however, there is evidence that differentiation in vitro differs from in vivo corticogenesis in several important aspects, such as the formation of six layers and the arealization in the cerebral cortex [5], suggesting that there are significant factors of neurogenesis missing from in vitro culture that are present in in vivo brain development.

Perhaps other extrinsic cues that exist only in vivo, such as the microenvironment generated by blood vessels [41] or the composition of the extracellular matrix [42], are also essential for the formation of the highly organized architecture of the mammalian cortex. Therefore, the robust incorporation of neurally induced ESCs using the TETCaD method would be an effective approach to fill in the gaps between neurogenesis from ESCs in vitro and the in vivo environment of the developing brain.

We demonstrated that human-ESC-derived cortical cells are robustly incorporated into the host mouse brain using the TETCaD method. One to 3 days after transplantation, human-ESC-derived cells are exclusively located in the VZ of the host cortex. Although these cells tend to be clustered without showing a clear polarity, single cells isolated from the cluster displayed apico-basally oriented processes, similar to endogenous mouse and human cortical progenitors. This result suggests that transplanted human cortical progenitors are capable of establishing apico-basal polarity by adapting to the extrinsic in vivo environment of the developing mouse cortex. Six days after transplantation, grafted human cells were dispersed throughout the cortical plate of the host mice. This result suggests that, even in the xenograft situation, human cortical neurons have the potential to migrate from the VZ to the cortical plate. This feature is evident when the host mouse brains were observed at a later time post-transplantation. In the P7 mouse cortex, human cells were scattered through cortical layers and displayed typical morphology of immature cortical pyramidal neurons. Taken together, our results demonstrate that the transplantation of human-ESC-derived cortical cells to the mouse embryonic cortex using the TETCaD method can be used as a model system to study human-specific features of cortical development that could not be studied solely in vitro. This approach may prove to be a very useful tool in the study of specific human neurodevelopmental diseases (such as microcephaly or lissencephaly) through the investigation of grafted iPSC-derived cortical cells from patients [43]. In addition, the TETCaD method could also be useful in defining human-specific mechanisms of cortical development that may be linked to the evolution of the human brain.

Acknowledgments

Author Disclosure Statement

No competing financial interests exist.

References

1. Gaspard N, T Bouschet, R Hourez, J Dimidschstein, G Naeije, J van den Ameele, I Espuny-Camacho, A Herpoel, L Passante, SN Schiffmann, et al. (2008). An intrinsic mechanism of corticogenesis from embryonic stem cells. Nature 455:351–357.

2. Shi Y, P Kirwan, J Smith, HP Robinson and FJ Livesey. (2012). Human cerebral cortex development from pluripotent stem cells to functional excitatory synapses. Nature Neurosci 15:477–486.S471.

3. Espuny-Camacho I, KA Michelsen, D Gall, D Linaro, A Hasche, J Bonnefont, C Bali, D Orduz, A Bilheu, A Herpoel, et al. (2013). Pyramidal neurons derived from human pluripotent stem cells integrate efficiently into mouse brain circuits in vivo. Neuron 77:440–456.

4. Eiraku M, K Watanabe, M Matsuo-Takasaki, M Kawada, S Yonemura, M Matsumura, T Wataya, A Nishiyama, K Muguruma and Y Sasai. (2008). Self-organized formation of polarized cortical tissues from ESCs and its active manipulation by extrinsic signals. Cell Stem Cell 3:519–532.

5. Gaspard N and P Vanderhaeghen. (2010). Mechanisms of neural specification from embryonic stem cells. Curr Opin Neurobiol 20:37–43.

6. Wernig M, F Benninger, T Schmandt, M Rade, KL Tucker, H Bussow, H Beck and O Brustle. (2004). Functional integration of embryonic stem cell-derived neurons in vivo. J Neurosci 24:5258–5268.

7. Lui JH, DV Hansen and AR Kriegstein. (2011). Development and evolution of the human neocortex. Cell 146:18–36.

8. Fietz SA and WB Huttner. (2011). Cortical progenitor expansion, self-renewal and neurogenesis-a polarized perspective. Curr Opin Neurobiol 21:23–35.

9. Noctor SC, AC Flint, TA Weissman, RS Dammerman and AR Kriegstein. (2001). Neurons derived from radial glial cells establish radial units in neocortex. Nature 409:714–720.

10. Miyata T, A Kawaguchi, H Okano and M Ogawa. (2001). Asymmetric inheritance of radial glial fibers by cortical neurons. Neuron 31:727–741.

11. Kosodo Y, K Toida, V Dubreuil, P Alexandre, J Schenk, E Kiyokage, A Attardo, F Mora-Bermudez, T Arii, JD Clarke, et al. (2008). Cytokinesis of neuroepithelial cells can divide their basal process before anaphase. EMBO J 27:3151–3163.

12. Shitamukai A, D Konno and F Matsuzaki. (2011). Oblique radial glial divisions in the developing mouse neocortex induce self-renewing progenitors outside the germinal zone that resemble primate outer subventricular zone progenitors. J Neurosci 31:3683–3695.

13. Noctor SC, V Martinez-Cerdeno, L Ivic and AR Kriegstein. (2004). Cortical neurons arise in symmetric and asymmetric division zones and migrate through specific phases. Nat Neurosci 7:136–144.

14. Miyata T, A Kawaguchi, K Saito, M Kawano, T Muto and M Ogawa. (2004). Asymmetric production of surface-dividing and non-surface-dividing cortical progenitor cells. Development 131:3133–3145.

15. Haubensak W, A Attardo, W Denk and WB Huttner. (2004). Neurons arise in the basal neuroepithelium of the early mammalian telencephalon: a major site of neurogenesis. Proc Natl Acad Sci U S A 101:3196–3201.

16. Hansen DV, JH Lui, PR Parker and AR Kriegstein. (2010). Neurogenic radial glia in the outer subventricular zone of human neocortex. Nature 464:554–561.

17. Fietz SA, I Kelava, J Vogt, M Wilsch-Brauninger, D Stenzel, JL Fish, D Corbeil, A Riehn, W Distler, R Nitsch, et al. (2010). OSVZ progenitors of human and ferret neocortex are epithelial-like and expand by integrin signaling. Nature Neurosci 13:690–699.

18. Wang X, JW Tsai, B LaMonica and AR Kriegstein. (2011). A new subtype of progenitor cell in the mouse embryonic neocortex. Nature Neurosci 14:555–561.

19. Reillo I, C de Juan Romero, MA Garcia-Cabezas and V Borrell. (2011). A role for intermediate radial glia in the tangential expansion of the mammalian cerebral cortex. Cereb Cortex 21:1674–1694.

20. Gaspard N, T Bouschet, A Herpoel, G Naeije, J van den Ameele and P Vanderhaeghen. (2009). Generation of cortical neurons from mouse embryonic stem cells. Nat Protoc 4:1454–1463.

21. Gassmann M, G Donoho and P Berg. (1995). Maintenance of an extrachromosomal plasmid vector in mouse embryonic stem cells. Proc Natl Acad Sci U S A 92:1292–1296.

22. Ying QL, M Stavridis, D Griffiths, M Li and A Smith. (2003). Conversion of embryonic stem cells into neuroectodermal precursors in adherent monoculture. Nat Biotech 21:183–186.

23. Toida K, K Kosaka, Y Aika and T Kosaka. (2000). Chemically defined neuron groups and their subpopulations in the glomerular layer of the rat main olfactory bulb—IV. Intraglomerular synapses of tyrosine hydroxylase-immunoreactive neurons. Neuroscience 101:11–17.

24. Nakamura K, H Hioki, F Fujiyama and T Kaneko. (2005). Postnatal changes of vesicular glutamate transporter (VGluT)1 and VGluT2 immunoreactivities and their colocalization in the mouse forebrain. J Comp Neurol 492:263–288.

25. Miyata T. (2008). Development of three-dimensional architecture of the neuroepithelium: role of pseudostratification and cellular 'community'. Dev Growth Differ 50 Suppl 1:S105–S112.

26. Mardia KV and PE Jupp. (2000). *Directional Statistics*. John Wiley & Sons Ltd, Chichester, p. 429.

27. Yoshida C and M Takeichi. (1982). Teratocarcinoma cell adhesion: identification of a cell-surface protein involved in calcium-dependent cell aggregation. Cell 28:217–224.

28. Rothen-Rutishauser B, FK Riesen, A Braun, M Gunthert and H Wunderli-Allenspach. (2002). Dynamics of tight and adherens junctions under EGTA treatment. J Membr Biol 188:151–162.

29. Wang XF, JZ Cui, SS Prasad and JA Matsubara. (2005). Altered gene expression of angiogenic factors induced by calcium-mediated dissociation of retinal pigment epithelial cells. Invest Ophthalmol Vis Sci 46:1508–1515.

30. Mirzadeh Z, FT Merkle, M Soriano-Navarro, JM Garcia-Verdugo and A Alvarez-Buylla. (2008). Neural stem cells confer unique pinwheel architecture to the ventricular surface in neurogenic regions of the adult brain. Cell Stem Cell 3:265–278.

31. Marin O, M Valiente, X Ge and LH Tsai. (2010). Guiding neuronal cell migrations. Cold Spring Harb Perspect Biol 2:a001834.

32. Kowalczyk T, A Pontious, C Englund, RA Daza, F Bedogni, R Hodge, A Attardo, C Bell, WB Huttner and RF Hevner. (2009). Intermediate neuronal progenitors (basal progenitors) produce pyramidal-projection neurons for all layers of cerebral cortex. Cereb Cortex 19:2439–2450.

33. Rakic P. (1972). Mode of cell migration to the superficial layers of fetal monkey neocortex. J Comp Neurol 145:61–83.

34. Fishell G. (1995). Striatal precursors adopt cortical identities in response to local cues. Development 121:803–812.

35. Brustle O, U Maskos and RD McKay. (1995). Host-guided migration allows targeted introduction of neurons into the embryonic brain. Neuron 15:1275–1285.

36. Campbell K, M Olsson and A Bjorklund. (1995). Regional incorporation and site-specific differentiation of striatal precursors transplanted to the embryonic forebrain ventricle. Neuron 15:1259–1273.

37. McConnell SK. (1988). Fates of visual cortical neurons in the ferret after isochronic and heterochronic transplantation. J Neurosci 8:945–974.

38. Spits C, C Le Caignec, M De Rycke, L Van Haute, A Van Steirteghem, I Liebaers and K Sermon. (2006). Whole-genome multiple displacement amplification from single cells. Nat Protoc 1:1965–1970.

39. Gaiano N and G Fishell. (1998). Transplantation as a tool to study progenitors within the vertebrate nervous system. J Neurobiol 36:152–161.

40. Tiberi L, P Vanderhaeghen and J van den Ameele. (2012). Cortical neurogenesis and morphogens: diversity of cues, sources and functions. Curr Opin Cell Biol 24:269–276.

41. Javaherian A and A Kriegstein. (2009). A stem cell niche for intermediate progenitor cells of the embryonic cortex. Cereb Cortex 19 Suppl 1:i70–i77.

42. Fietz SA, R Lachmann, H Brandl, M Kircher, N Samusik, R Schroder, N Lakshmanaperumal, I Henry, J Vogt, A Riehn, et al. (2012). Transcriptomes of germinal zones of human and mouse fetal neocortex suggest a role of extracellular matrix in progenitor self-renewal. Proc Natl Acad Sci U S A 109:11836–11841.

43. Saporta MA, M Grskovic and JT Dimos. (2011). Induced pluripotent stem cells in the study of neurological diseases. Stem Cell Res Ther 2:37.

Address correspondence to:
Dr. Yoichi Kosodo
Department of Anatomy
Kawasaki Medical School
577 Matsushima
Kurashiki 701-0192
Japan

E-mail: kosodo@med.kawasaki-m.ac.jp